Cement and Concrete Research 40 (2010) 1441–1450

Contents lists available at ScienceDirect

Cement and Concrete Research

journal homepage: http://ees.elsevier.com/CEMCON/default.asp

Effects of non-uniform corrosion on the cracking and service life of reinforced concrete structures

Bong Seok Jang [a], Byung Hwan Oh [b,*]

[a] Korea Institute of Water and Environment, KWATER, Daejeon, Republic of Korea
[b] Seoul National University, Gwanak-gu, Seoul, Republic of Korea

ARTICLE INFO

Article history:
Received 6 September 2009
Accepted 18 March 2010

Keywords:
Non-uniform corrosion
Concrete cover
Cracking pressure
Service life
Durability

ABSTRACT

The purpose of this study is to explore the effects of non-uniform corrosion on cracking behavior of concrete cover. The effects of non-uniform corrosion distribution, cover-to-rebar diameter ratio, and concrete compressive strength on the cracking pressure of concrete cover were studied. The present study indicates that the pressures to cause cracking of concrete cover under non-uniform corrosion conditions are much smaller than those under uniform corrosion case. The cracking pressure decreases up to about 60% depending upon the types of non-uniform corrosion distributions. It was also shown that cover-to-rebar diameter ratio and concrete compressive strength affect greatly the cracking pressure of concrete cover. Realistic equations on the cracking pressure of concrete cover were derived. The comparisons of analysis results with the test data on the cracking pressure of concrete cover show fairly good agreement. Finally, the effect of non-uniform corrosion on the service life of concrete structures was discussed.

1. Introduction

Reinforced concrete structures exposed to sea environments may suffer from corrosion of steel bars due to chloride ingress [1–7]. Chloride ingress is, therefore, a major factor that affects durability of concrete structures [8–17]. The corrosion products of a reinforcing bar in concrete induce pressure to the surrounding concrete due to the expansion of corroded steel. This expansion pressure induces tensile stresses in concrete around the reinforcing bar and the continuous increase of expansion pressure eventually causes cracking through concrete cover [18–21]. The cracking of concrete cover due to steel corrosion may accelerate corrosion process and lead to failure very rapidly. Therefore, corrosion-induced cracking of concrete cover is an important and essential problem in concrete structures because it directly affects not only durability, but also service life of such structures.

In this regard, the authors have conducted a series of corrosion tests in order to determine the critical corrosion amounts which cause the cracking of concrete cover [19]. The authors also proposed an advanced model on the relation between corrosion-induced expansion pressure and corrosion layer strain in reinforced concrete members [20]. It has been generally assumed for simple application that corrosion occurs uniformly and thus expansion pressure is uniform around a rebar [5]. However, since chlorides are penetrated in one direction in actual sea environments, the corrosion may start from the most-outer part of the rebar and thus the steel bar may not corrode uniformly in a cross section. This can be more emphasized from the authors' previous study [5] that the chlorides are accumulated in front of rebar because the chlorides do not diffuse through the rebar. This means that real state of corrosion is not uniform around a rebar and starts from pitting corrosion [17]. This causes non-uniform expansion pressure around the rebar.

The purpose of the present study is therefore to explore the effects of non-uniform corrosion on cracking behavior of concrete cover. Non-uniform distribution of expansion pressure may cause adverse effects for the cracking of concrete cover because higher pressure is concentrated at the outer region of rebar toward concrete cover. This may cause higher tensile stress development and fast occurrence of cracks in concrete cover which reduces time-to-cracking and eventually service life of concrete structures [22–24]. This is an important problem in analysis of corrosion-induced cracking and failure of concrete.

2. State of non-uniform corrosion

Since chlorides are penetrated in one direction in real sea environments, corrosion may start from the outer region of a rebar and thus the steel bar may not corrode uniformly around the rebar. Fig. 1 shows the cases of uniform and non-uniform corrosion around a rebar. D_0 in Fig. 1 indicates the initial diameter of rebar before corrosion and D_t represents the diameter of rebar at the current time after loosing some steel cross-sections due to corrosion. For the case of non-uniform corrosion in the right side of Fig. 1, it may be reasonably assumed that the corrosion depth of steel bar is linearly decreased

* Corresponding author.
E-mail address: bhohcon@snu.ac.kr (B.H. Oh).

0008-8846/$ – see front matter © 2010 Elsevier Ltd. All rights reserved.
doi:10.1016/j.cemconres.2010.03.018

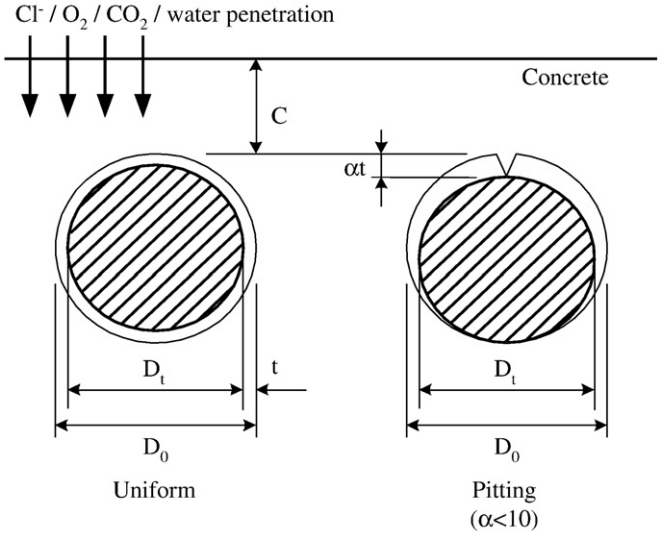

Fig. 1. Basic description for uniform and non-uniform corrosion distributions.

from the outer region of the rebar. The value of α in Fig. 1 is defined as the ratio of the depth of non-uniform corrosion to that of uniform corrosion. It was reported from the experiments of González et al [25] that the value α ranges about 4–8 in natural conditions and 5–13 in accelerated testing of reinforced concrete, and is usually less than about 10.

3. Nonlinear analyses of concrete cover due to non-uniform corrosion distributions

3.1. Analysis variables for uniform and non-uniform corrosion distributions around a steel bar

As explained in the previous section, the appropriate values of α considered in this study were ranged from 1 to 8 in order to explore the effects of non-uniform corrosion distributions on the cracking behavior of concrete cover in reinforced concrete members. The various corrosion distributions for these cases are depicted in Fig. 2 depending upon the values of α. Major variables for analyses were the types of nonlinear corrosion distributions ($\alpha = 1, 2, 4, 8$), diameter of rebar (8 mm[0.32 in.], 16 mm[0.64 in.]), cover depth-to-rebar diameter ratio ($c/d = 0.5, 1.0, 2.0$), and compressive strengths of concrete (20.6 MPa [3.0 ksi]), 27.5 MPa [4.0 ksi], and 44.1 MPa [6.4 ksi]), respectively. Three different compressive strengths of concrete were considered to examine the effect of concrete strength on the cracking behavior due to corrosion. The corresponding Young's moduli, E_c, were 21.5 GPa (3120 ksi), 24.8 GPa (3600 ksi), and 31.4 GPa (4560 ksi), respectively. The location of rebar in concrete members, namely side rebar or corner rebar, was also considered to see the effect of rebar locations.

3.2. Material models for nonlinear analysis

To model concrete, eight-node plane strain elements were used. For the compressive regime of concrete, Mohr–Coulomb failure model was applied where cohesion c was calculated as follows.

$$c = \frac{1-\sin\phi}{2\cos\phi} \tag{1}$$

Here, the friction angle ϕ is approximately 30° for concrete. For the tensile regime, the smeared crack concept was employed to model cracking of concrete elements. A crack arises if the major principal tensile stress exceeds the minimum of tensile strength f_t and $f_t(1+\sigma_{\text{lateral}}/f_c)$, where the lateral principal stress σ_{lateral} considers the effect of biaxial stress. The direct tensile strength $f_t$of concrete may also be obtained from the split tensile strength f_{sp} and compressive strength f_c as shown in Eqs. (2) and (3) [26].

$$f_{sp} = 0.2 f_c^{0.7} \text{ MPa} \tag{2}$$

$$f_c = 0.9 f_{sp} \text{ MPa}. \tag{3}$$

For tension softening, bilinear tension softening model according to Hillerborg [27] was used as shown in Fig. 3. The value of fracture energy G_F was reasonably assumed as 100 N/m (0.571 lb/in) for the present analysis which is a typical value in concrete [27].

3.3. Solution scheme of nonlinear analysis

In order to analyze the nonlinear relation between load and displacement, an incremental iterative solution procedure is required. The equilibrium based on internal energy is iteratively achieved within each increment. In this study, convergence criterion was taken as the ratio of internal energy between two successive load steps and the tolerance, namely convergence criterion, was assigned to be 1×10^{-2}. Iteration is repeated until internal equilibrium conditions are fulfilled and convergence is obtained. The regular Newton–Raphson method was applied for iteration procedure in which stiffness matrix is evaluated at every iteration. Fig. 4(a) illustrates the iteration procedure of regular Newton–Raphson method. However, for descending parts after maximum load level, the Newton–Raphson method cannot find next load level. Therefore, Arc-length method was utilized as shown in Fig. 4(b) for this region. This method makes it possible to find the next load step using predefined arc length at each step. With this path-following technique, the post-peak descending part has been reasonably investigated.

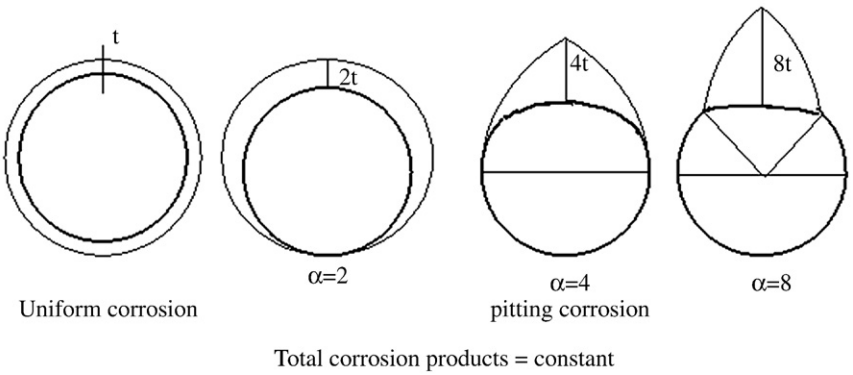

Fig. 2. Various types of corrosion distribution for $\alpha = 1$, 2, 4, and 8, respectively.

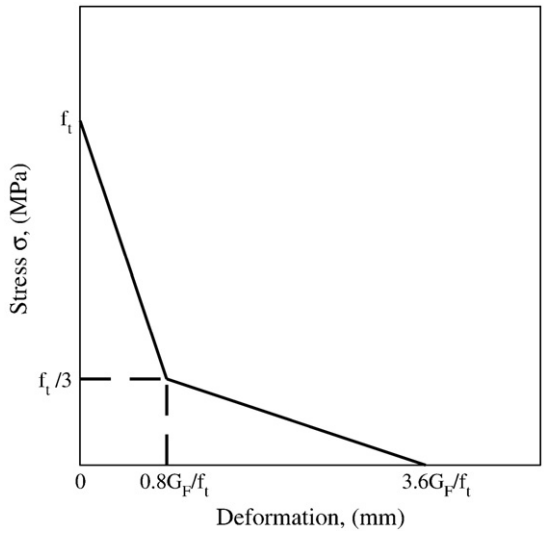

Fig. 3. Bilinear tension softening curve of concrete.

3.4. Finite element analysis models

Fig. 5 shows the finite element meshes for the nonlinear analysis of concrete members due to corrosion-induced expansion pressure for side located rebar. Fig. 6 shows the finite element meshes for corner located rebar. The identification of analysis variables was summarized in Fig. 7. For example, the identification variable M-f_{c1}-$D8$-Cd0.5-α_1 represents the case of middle side-located rebar (M), compressive strength $f_{c1}=f_c=20.6$ MPa (3.0 ksi), rebar diameter $d=8$ mm (0.32 in.), cover-to-rebar diameter ratio $c/d=0.5$, and uniform corrosion $\alpha=1$ (see Fig. 7), and also the identification variable M-f_{c2}-$D16$-Cd1.0-α_2 represents the case of middle side-located rebar (M), compressive strength $f_{c2}=f_c=27.5$ MPa (4.0 ksi), rebar diameter $d=16$ mm (0.64 in.), cover-to-rebar diameter ratio $c/d=1.0$, and non-uniform corrosion $\alpha=2$ (see Fig. 7).

3.5. Corrosion-induced pressure distributions for nonlinear analysis

Fig. 8 shows the distributions of corrosion-induced expansion pressure around a rebar used in this study. This was deduced from the non-linear corrosion distributions according to the value of α already explained in Fig. 2. Fig. 8 shows only the enlarged portion around a rebar in the finite element analysis. The internal pressure distributions shown in Fig. 8 were applied to the surrounding concrete in an incremental manner up to the crack occurrence of concrete cover.

4. Analysis of results

4.1. Cracking pressures of concrete cover

The analysis results on the cracking pressures of concrete cover for various cases were summarized in Tables 1–3. The cracking pressure was defined here as the expansion pressure at which the cracking occurs first on the surface region of concrete cover during the step-by-step incremental nonlinear analysis. Table 1 shows the cracking pressures of concrete cover according to various design parameters for the case of concrete compressive strength $f_c=20.6$ MPa (3.0 ksi). Tables 2 and 3 exhibit the similar results according to various design parameters for the cases of concrete compressive strength $f_c=27.5$ MPa (4.0 ksi) and 44.1 MPa (6.4 ksi), respectively.

Table 1 indicates that the cracking pressure decreases greatly as the corrosion distribution becomes sharper, i.e., the value of α for non-uniform corrosion becomes larger (see Fig. 2). The cracking pressures for non-uniform corrosion $\alpha=4$ and 8 are about 60% and 40% of that for uniform corrosion case, respectively. This means that the cracking of concrete cover due to corrosion of steel bar occurs much earlier when the corrosion is localized at the outer region of rebar. This is the case of usual pitting corrosion occurring in actual concrete structures under sea environments [25]. Table 1 also shows that the depth of concrete cover affects greatly the cracking pressures as expected.

4.2. Effect of non-uniform corrosion distribution

Fig. 9 depicts the effect of non-uniform corrosion on the cracking pressure (P_{cr}) of concrete cover and also the stress distribution (in MPa) in concrete around a steel bar for the case of middle-side rebar (M), compressive strength $f_c=27.5$ MPa (4 ksi), cover depth $d=8$ mm (0.32 in.), and cover-to-diameter ratio $c/d=1.0$ (M-f_{c2}-$D8$-Cd1.0). The values in the legend of Fig. 9 represent the stresses (in MPa) in concrete arising from internal pressure distribution of Fig. 8. Fig. 9 indicates that the cracking pressures for $\alpha=1$(uniform corrosion) and $\alpha=2$(mild non-uniform corrosion) are almost same and do not show much difference. However, the cracking pressures for $\alpha=4$ and $\alpha=8$ (medium and severe non-uniform corrosions) are much smaller than that of uniform corrosion case, namely 40% and 60% decrease of cracking

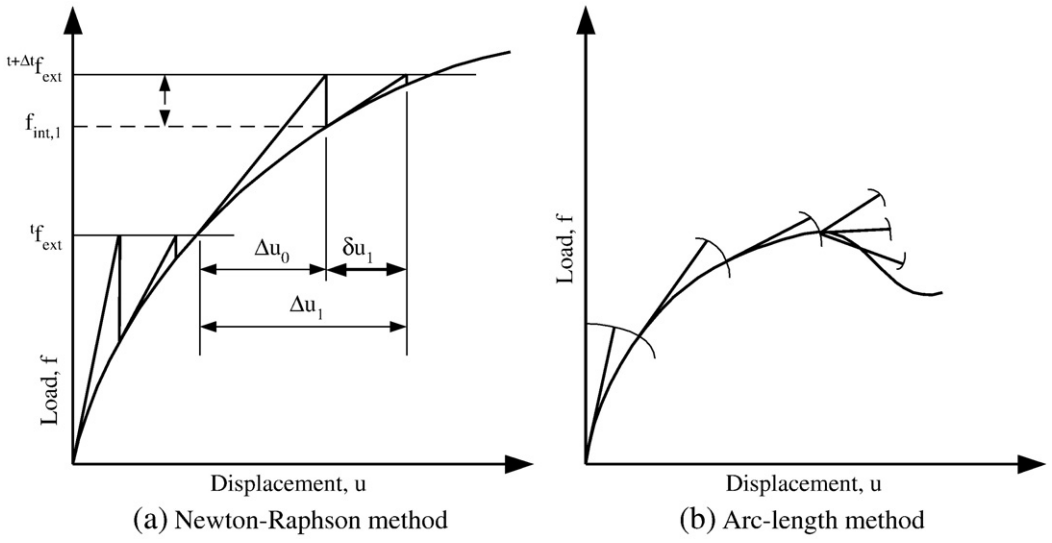

Fig. 4. Solution schemes for nonlinear analysis.

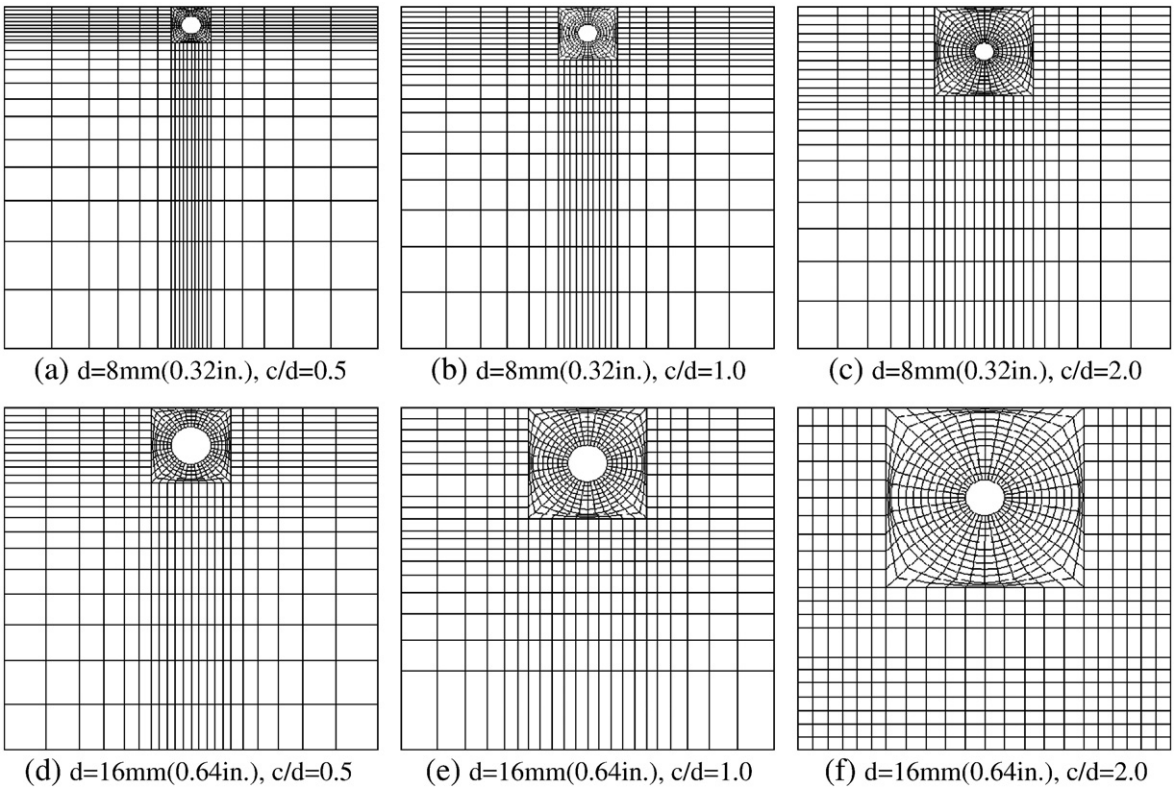

Fig. 5. Finite element meshes for various cover-to-rebar diameter (c/d) values for middle side-located rebar.

pressure, respectively. This means that a local corrosion in relatively small area at the outer face of rebar can cause the failure of concrete cover at a relatively low expansion pressure in case of pitting corrosion. This gives important implications in actual practice because the corrosion in real structures is usually of pitting and non-uniform nature. González et al [25] reported that the value of α ranges about 4–8 in natural corrosion conditions. It is therefore noted here that the corrosion distribution is a very important factor in corrosion-induced failure of

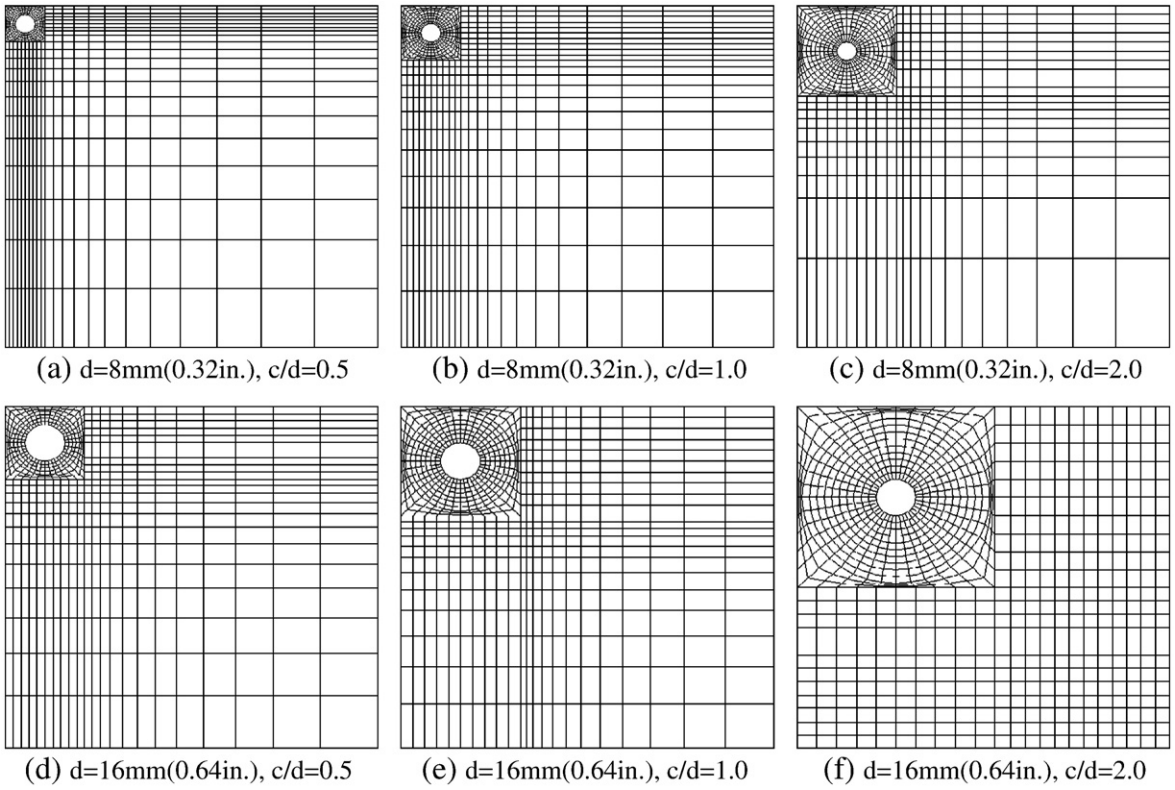

Fig. 6. Finite element meshes for various cover-to-rebar diameter (c/d) values for corner-located rebar.

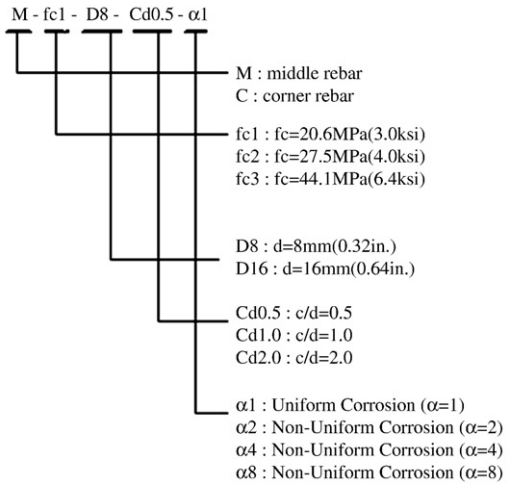

Fig. 7. Identification for analysis variables.

concrete cover which affects directly the durability as well as service life of concrete structures. Fig. 10 summarizes the regression equations for cracking pressures in terms of α value for various c/d ratios for the case of middle-side rebar, $f_c = 27.5$ MPa(4 ksi), and rebar diameter $d = 16$ mm(0.64 in.). The following equations were derived from the analysis results.

$$P_{cr} = 1.585\ \alpha^{-0.50} \quad \text{for } c/d = 0.5 \tag{4}$$

$$P_{cr} = 3.303\ \alpha^{-0.45} \quad \text{for } c/d = 1.0 \tag{5}$$

$$P_{cr} = 6.703\ \alpha^{-0.40} \quad \text{for } c/d = 2.0 \tag{6}$$

where P_{cr} = corrosion-induced expansion pressure to cause cracking of concrete cover in MPa (1 MPa = 145 psi), c/d = cover-to-rebar diameter ratio, and $\alpha \geq 1$. The above equations may be efficiently used to calculate the cracking pressures due to corrosion for normal strength concrete of around 27.5 Mpa (4 ksi).

4.3. Effect of cover depth

Fig. 11 shows the effect of cover depth on the cracking pressure (P_{cr}) and the stress distribution (in MPa) in concrete around a steel bar for the case of middle-side rebar (M), compressive strength $f_c = 27.5$ MPa (4 ksi), cover depth $d = 8$ mm (0.32 in.), and uniform corrosion $\alpha = 1$ (M-f_{c2}-$D8$-α_1). Fig. 11 indicates that the cracking pressures for $c/d = 0.5$, 1.0, and 2.0 are 1.4 MPa (203 psi), 2.95 MPa (428 psi), and 5.96 MPa (864 psi), respectively. Fig. 12 expresses the cracking pressure as a function of cover-to-rebar diameter (c/d) ratio for various bar diameters and α values (the case of middle-side rebar, $f_c = 27.5$ MPa (4 ksi)). Fig. 12 indicates that the pressure to cause cracking of concrete cover due to corrosion expansion increases with an increase of cover depth and is linearly proportional to the cover depth-to-rebar diameter (c/d) ratio as follows.

$$P_{cr} = 2.845(c/d)^{1.05} \quad \text{for} \alpha = 1 \tag{7}$$

$$P_{cr} = 1.693\ (c/d)^{1.11} \quad \text{for} \alpha = 4 \tag{8}$$

Here P_{cr} represents the pressure (in MPa; 1 MPa = 145 psi) to cause cracking of concrete cover due to corrosion expansion and c/d is cover depth-to-rebar diameter ratio. The correlation coefficient is almost 1 as

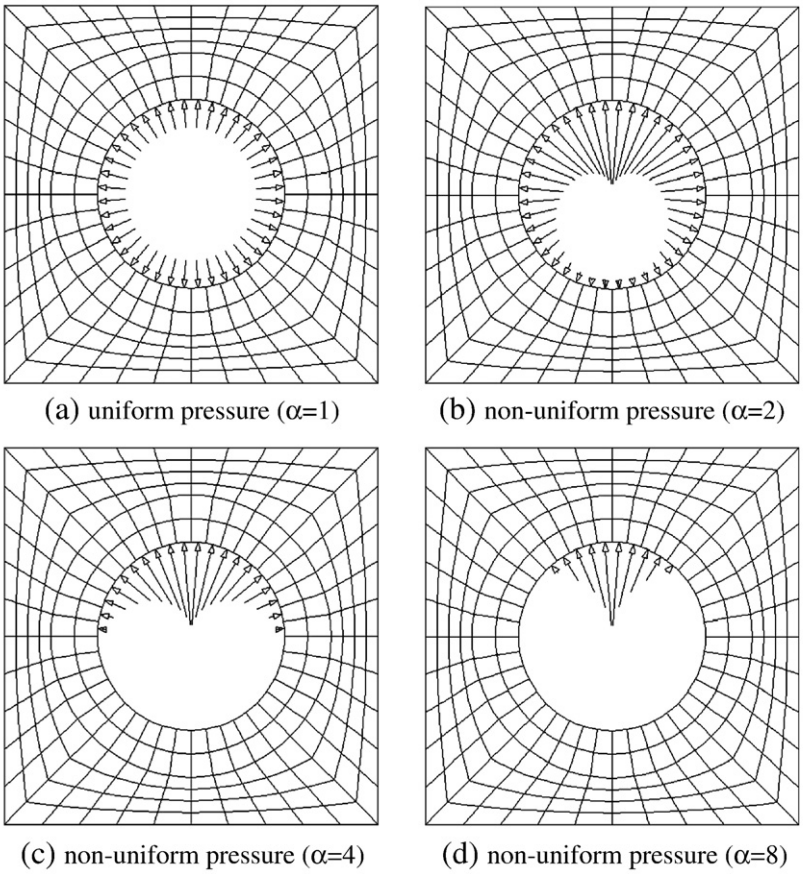

Fig. 8. Uniform and non-uniform pressure distributions around a rebar (enlarged diagrams only around a rebar).

Table 1
Cracking pressures for uniform and non-uniform corrosion conditions [f_c = 20.6 MPa(3.0 ksi)].

	Rebar dia.; d mm(in)	Cover depth; c mm(in)	c/d ratio	Types of corrosion distribution MPa (psi)			
				$\alpha=1$	$\alpha=2$	$\alpha=4$	$\alpha=8$
Middle side rebar	8 (0.32)	4 (0.16)	0.5	1.14 (165)	1.16 (168)	0.64 (93)	0.44 (64)
		8 (0.32)	1.0	2.41 (349)	2.46 (357)	1.39 (202)	1.00 (145)
		16 (0.64)	2.0	4.88 (708)	5.11 (741)	2.90 (421)	2.19 (318)
	16 (0.64)	8 (0.32)	0.5	1.11 (161)	1.14 (165)	0.62 (90)	0.42 (61)
		16 (0.64)	1.0	2.33 (338)	2.44 (354)	1.38 (200)	1.00 (145)
		32 (1.28)	2.0	4.78 (693)	5.13 (744)	3.00 (435)	2.22 (322)
Corner side rebar	8 (0.32)	4 (0.16)	0.5	1.12 (162)	1.26 (183)	0.62 (90)	0.40 (58)
		8 (0.32)	1.0	2.52 (365)	2.73 (396)	1.47 (213)	1.00 (145)
		16 (0.64)	2.0	5.10 (739)	5.62 (814)	3.22 (467)	2.37 (344)
	16 (0.64)	4 (0.16)	0.5	1.20 (174)	1.24 (180)	0.62 (90)	0.40 (58)
		8 (0.32)	1.0	2.50 (363)	2.71 (393)	1.46 (212)	0.96 (139)
		16 (0.64)	2.0	5.07 (735)	5.44 (789)	3.13 (454)	2.30 (334)

Table 2
Cracking pressures for uniform and non-uniform corrosion conditions [f_c = 27.5 MPa(4.0 ksi)].

	Rebar dia.; d mm(in)	Cover depth; c mm(in)	c/d ratio	Types of corrosion distribution MPa (psi)			
				$\alpha=1$	$\alpha=2$	$\alpha=4$	$\alpha=8$
Middle side rebar	8 (0.32)	4 (0.16)	0.5	1.40 (203)	1.44 (209)	0.78 (113)	0.54 (78)
		8 (0.32)	1.0	2.95 (428)	3.05 (442)	1.71 (248)	1.23 (178)
		16 (0.64)	2.0	5.96 (864)	6.20 (899)	3.59 (521)	2.74 (397)
	16 (0.64)	8 (0.32)	0.5	1.37 (199)	1.40 (203)	0.78 (113)	0.52 (75)
		16 (0.64)	1.0	2.87 (416)	3.03 (439)	1.70 (247)	1.22 (177)
		32 (1.28)	2.0	5.86 (850)	6.33 (918)	3.66 (531)	2.76 (400)
Corner side rebar	8 (0.32)	4 (0.16)	0.5	1.49 (216)	1.54 (223)	0.76 (110)	0.50 (73)
		8 (0.32)	1.0	3.10 (450)	3.36 (487)	1.79 (260)	1.23 (178)
		16 (0.64)	2.0	6.29 (912)	6.87 (996)	3.93 (570)	2.91 (422)
	16 (0.64)	4 (0.16)	0.5	1.48 (215)	1.52 (220)	0.76 (110)	0.48 (70)
		8 (0.32)	1.0	3.08 (447)	3.33 (483)	1.78 (258)	1.26 (183)
		16 (0.64)	2.0	6.20 (899)	6.75 (979)	3.81 (552)	2.84 (412)

shown in Fig. 12 which represents almost perfect correlation between cracking pressure and cover-to-rebar diameter ratios.

4.4. Effect of rebar diameter

Tables 1–3 show the cracking pressures for two different rebar diameters for various compressive strengths and various c/d ratios. It can be clearly seen here that the cracking pressure decreases slightly as bar diameter increases. However, the difference is very small and it may be said that the bar diameter does not affect much for the pressures to cause cracking of concrete cover.

4.5. Effect of concrete strength

Fig. 13 shows the effect of concrete strength on the cracking pressure (P_{cr}) and the stress distribution (in MPa) in concrete around a steel bar for the case of middle-side rebar (M), rebar diameter d = 8 mm(0.32 in.), cover-to-rebar diameter ratio c/d = 0.5, and non-uniform corrosion $\alpha=2$(M-D8-Cd0.5-α_2). Fig. 13 indicates that the cracking pressure increases as concrete strength increases. Fig. 14 summarizes the cracking pressures as a function of compressive strength for various α values (non-uniform corrosion) for the case of middle-side rebar and d = 16 mm (0.64 in.). It can be seen from

Table 3
Cracking pressures for uniform and non-uniform corrosion conditions [f_c = 44.1 MPa(6.4 ksi)].

	Rebar dia.; d mm(in)	Cover depth; c mm(in)	c/d ratio	Types of corrosion distribution MPa (psi)			
				$\alpha=1$	$\alpha=2$	$\alpha=4$	$\alpha=8$
Middle side rebar	8 (0.32)	4 (0.16)	0.5	1.95 (283)	2.00 (290)	1.12 (162)	0.74 (107)
		8 (0.32)	1.0	4.12 (597)	4.24 (615)	2.35 (341)	1.67 (242)
		16 (0.64)	2.0	8.32 (1206)	8.72 (1264)	5.09 (738)	3.76 (545)
	16 (0.64)	8 (0.32)	0.5	1.90 (276)	1.94 (281)	1.06 (154)	0.72 (104)
		16 (0.64)	1.0	4.00 (580)	4.20 (609)	2.45 (355)	1.70 (247)
		32 (1.28)	2.0	8.01 (1161)	8.72 (1264)	5.06 (734)	3.83 (555)
Corner side rebar	8 (0.32)	4 (0.16)	0.5	2.06 (299)	2.14 (310)	1.06 (154)	0.80 (116)
		8 (0.32)	1.0	4.32 (626)	4.68 (678)	2.58 (374)	1.97 (286)
		16 (0.64)	2.0	8.72 (1264)	9.52 (1380)	5.42 (786)	4.17 (605)
	16 (0.64)	4 (0.16)	0.5	2.04 (296)	2.12 (307)	1.06 (154)	0.78 (113)
		8 (0.32)	1.0	4.28 (621)	4.64 (673)	2.44 (354)	1.95 (283)
		16 (0.64)	2.0	8.24 (1195)	9.20 (1334)	5.32 (771)	4.06 (589)

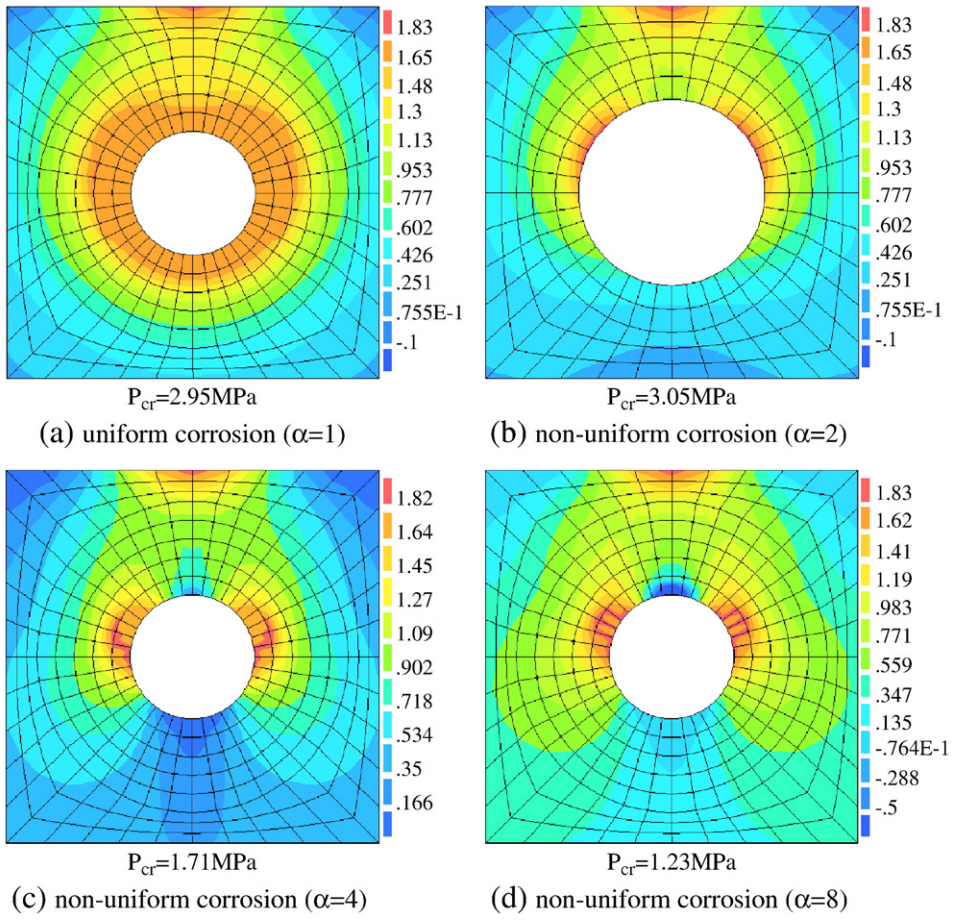

Fig. 9. Effect of non-uniform corrosion on the cracking pressure P_{cr} and stress distribution around a steel bar for the case of *M-f*$_{c2}$*-D*8-Cd1.0 (middle-side rebar, f_c = 27.5 MPa (4 ksi), d = 8 mm (0.32 in.), c/d = 1.0) [note: red, orange and yellow colors represent tensile stresses, the pale blue nearly zero stress and the dark blue a compressive stress].

Fig. 14 that there exists fairly good correlation between cracking pressure and compressive strength and that the cracking pressure is proportional to the (2/3) power of compressive strength. Fig. 14 also indicates that cracking pressure becomes much smaller as the distribution of non-uniform corrosion becomes sharper.

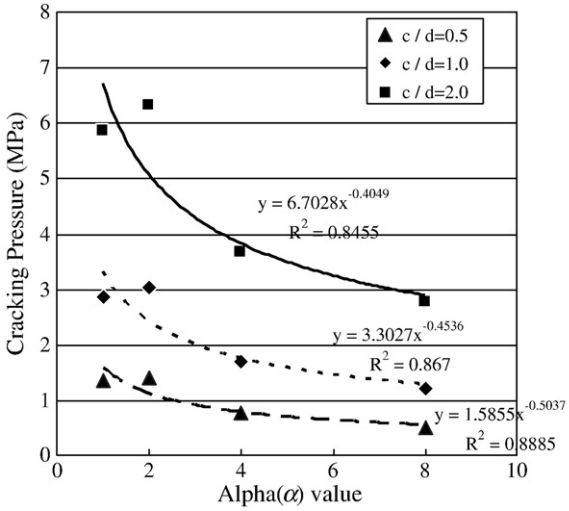

Fig. 10. Variation of cracking pressures depending on α value(non-uniform corrosion) and c/d ratios for middle-side rebar, f_c = 27.5 MPa(4 ksi), and bar diameter 6 mm (0.64 in.) (*M-f*$_{c2}$*-D*16) [dual unit: 1 MPa = 145 psi].

$$P_{cr} = 0.619 f_c^{0.68} \text{ for } d = 16\text{mm}(0.64\text{in.}) \text{ and } \alpha = 1 \quad (9)$$

$$P_{cr} = 0.376 f_c^{0.68} \text{ for } d = 16\text{mm}(0.64\text{in.}) \text{ and } \alpha = 4 \quad (10)$$

$$P_{cr} = 0.257 f_c^{0.71} \text{ for } d = 16\text{mm}(0.64\text{in.}) \text{ and } \alpha = 8 \quad (11)$$

where P_{cr} = corrosion-induced expansion pressure to cause cracking of concrete cover in MPa (1 MPa = 145 psi), f_c = compressive strength of concrete in MPa (1 MPa = 145 psi).

4.6. Comparison of analysis results with test data

Williamson and Clark [21] conducted a series of test to explore the internal pressure which is required to cause cracking of concrete cover due to reinforcement corrosion. Tests were carried out to investigate the magnitude of pressure created by corrosion products on steel in reinforced concrete that would cause surface cracking of the concrete cover. The present analysis results were compared with Williamson and Clark's test data [21].

Fig. 15 shows the comparison of present analysis results with Williamson and Clark's test data on cracking pressures according to c/d ratio for rebar diameter of 8 mm (0.32 in.) and 16 mm (0.64 in.), respectively. It is noted here that the analysis results correlate very well with test data as shown in Fig. 15.

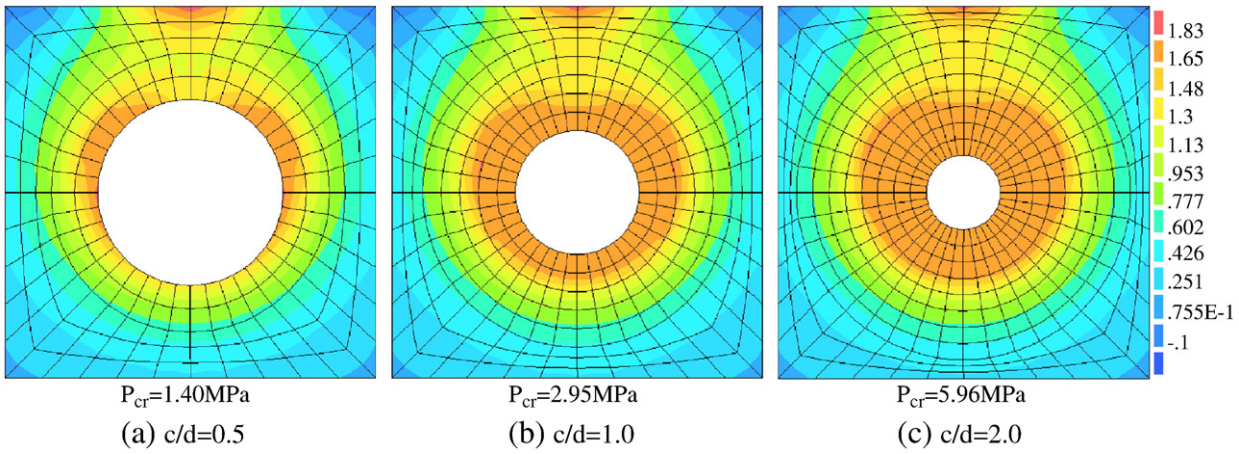

Fig. 11. Effect of cover depth on the cracking pressure P_{cr} and stress distribution around a steel bar for the case of *M*-f_{c2}-*D*8-α_1 (middle-side rebar, $f_c = 27.5$ MPa (4 ksi), $d = 8$ mm (0.32 in.), uniform corrosion $\alpha = 1$) [note: c/d = cover-to-rebar diameter ratio; red, orange and yellow colors represent tensile stresses, the pale blue nearly zero stress and the dark blue a compressive stress].

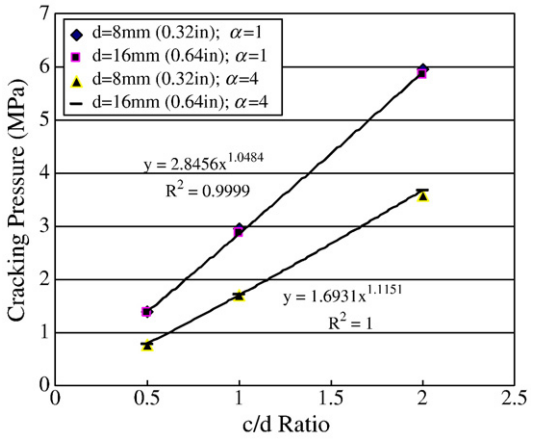

Fig. 12. Cracking pressure as a function of cover-to-rebar diameter (c/d) ratio for various bar diameters and α values [the case of middle-side rebar, $f_c = 27.5$ MPa (4 ksi)] (dual unit: 1 MPa = 145 psi).

5. Application to service life prediction

Penetrated chlorides into concrete are accumulated in front of reinforcing bar in concrete under sea environment. If the accumulated chlorides exceed a certain critical value, then the steel bar starts to corrode [5]. This critical value of chlorides is called the "threshold value" for corrosion initiation [6,8–10]. The life time or service life of concrete structures may be reasonably defined as the time to corrosion initiation plus time to cracking (cover failure). The authors reported in a recent study[5] that existence of steel bar must be considered in chloride diffusion analysis to obtain realistically accumulated chlorides in front of rebar. This allows more accurate determination of the time to corrosion initiation. It was found from the authors' recent study[5] that the time to corrosion initiation reduces by about 30–40% when the existence of reinforcing bar is considered in the accurate diffusion analysis. This is because chloride diffusion does not occur through the reinforcing bar itself and thus the chlorides are accumulated in front of a reinforcing bar. Fig. 16 depicts one of the results from the authors' study [5] which shows the chloride profiles penetrated into concrete for the case of rebar diameter $d = 20$ mm(0.8 in.) and cover thickness $c = 20$ mm(0.8 in.). An important finding here is that the chlorides accumulate in front of the reinforcing bar and that it shows much higher chlorides values at the location of rebar, compared with those without considering

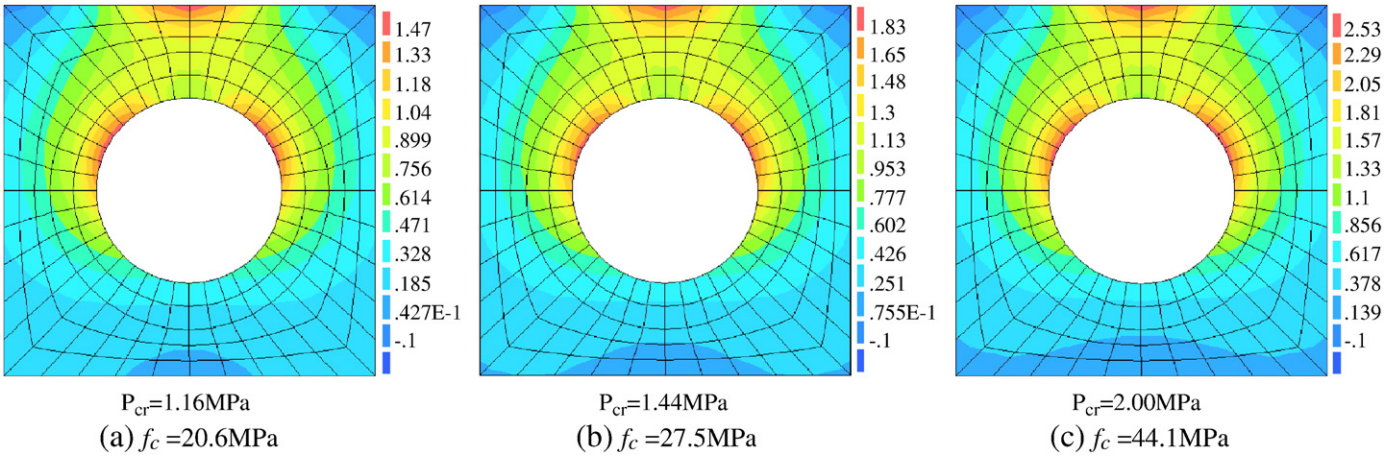

Fig. 13. Effect of concrete strength on the cracking pressure P_{cr} and stress distribution around a steel bar for the case of *M*-*D*8-Cd0.5-α_2 (middle-side rebar, $d = 8$ mm(0.32 in.), c/d = cover-to-rebar diameter ratio = 0.5, non-uniform corrosion $\alpha = 2$) [note: red, orange and yellow colors represent tensile stresses, the pale blue nearly zero stress and the dark blue a compressive stress].

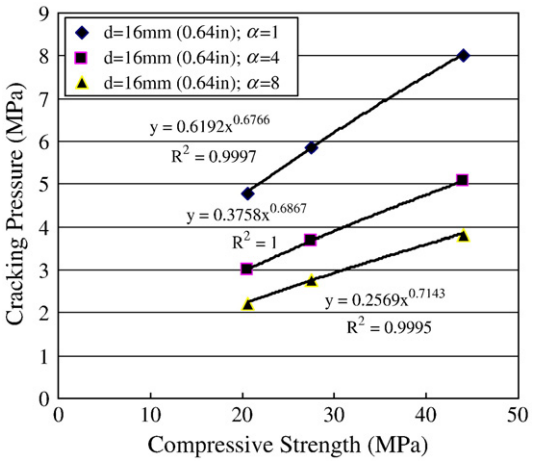

Fig. 14. Cracking pressure as a function of compressive strength for various α values (non-uniform corrosion) [the case of middle-side rebar and $d = 16$ mm (0.64 in.)] [dual unit: 1 MPa = 145 psi].

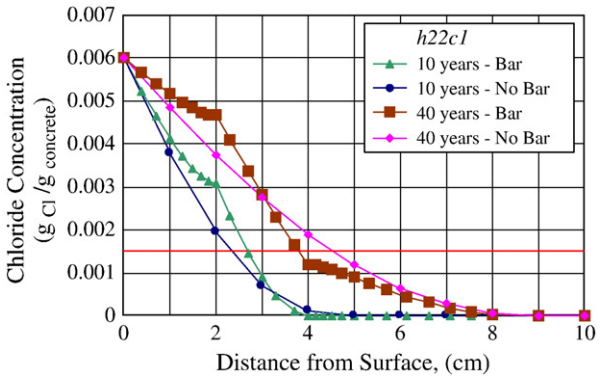

Fig. 16. Penetrated chloride profiles along the depth with or without considering reinforcing bar after 10 and 40 years, respectively[the case of bar diameter = 20 mm (0.8 in.), cover depth = 20 mm (0.8 in.)] (dual unit: 2 cm = 0.8in).

reinforcement. This higher accumulation of chloride in front of reinforcing bar may cause faster corrosion of reinforcing steel and thus reduce the lifetime of the structures.

As for the time to cracking of concrete cover after corrosion initiation, it may be also inferred from the analysis results in Tables 1–3 and Figs. 9–10. Tables 1–3 indicate that the cracking pressures for non-uniform corrosion $\alpha = 4$ and $\alpha = 8$ are about 60% and 40% of that for uniform corrosion case, respectively. This means that the cracking of concrete cover due to corrosion of steel bar occurs much earlier when the corrosion is localized at the outer region of rebar, which represents more real situation as reported by González et al [25].

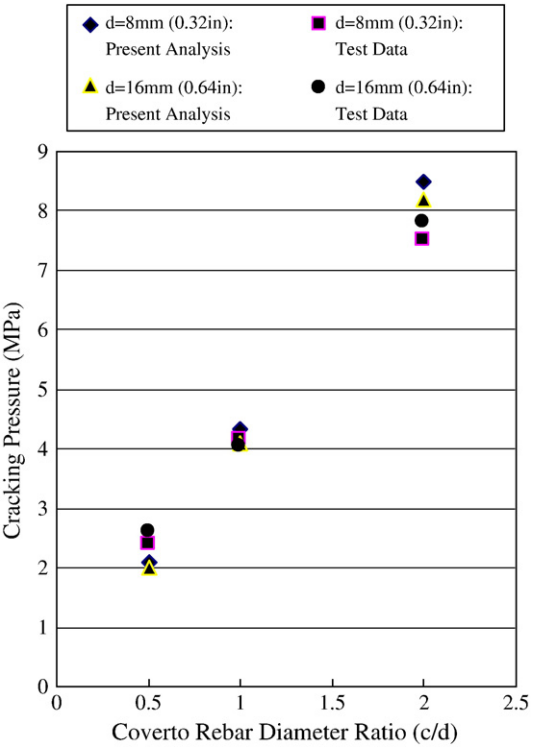

Fig. 15. Comparison of present analysis results with Williamson and Clark's test data on cracking pressures according to c/d ratio [dual unit: 1 MPa = 145 psi].

Therefore, the life time or service life which is defined as the sum of time-to-corrosion initiation plus time-to-cover cracking decreases greatly if one considers realistically the effect of rebar in chloride diffusion analysis and the effect of non-uniform corrosion distribution in cracking analysis.

6. Conclusions

Corrosion of steel bars in concrete may be the most dominant factor which affects durability and service life of concrete structures. The corrosion of steel bar in concrete may cause expansion pressure and this expansion pressure may then induce tensile cracking around the reinforcing bar. Since chlorides are generally penetrated into concrete in one direction under actual sea environments, the corrosion may start from the outermost part of the rebar and thus the steel bar may not corrode uniformly in a cross section, which has been also reported by the experimental study of González et al [25]. The purpose of the present study is therefore to explore the effects of non-uniform corrosion on the cracking behavior of concrete cover. Non-uniform distribution of expansion pressure may cause adverse effects for the cracking of concrete cover because higher pressure is concentrated at the outer region of rebar toward concrete cover. The following conclusions were drawn from the present study.

1. The pressures to cause cracking of concrete cover under non-uniform corrosion conditions ($\alpha = 4$–8) are much smaller than that of uniform corrosion case. Namely, the cracking pressure decreases up to 40%–60% depending upon the type of non-uniform corrosion distribution. This means that a local corrosion at the outer face of rebar can cause the failure of concrete cover at a relatively low expansion pressure. It was reported from the experiments of González et al [22] that the value α (the degree of non-uniform corrosion) ranges about 4–8 in natural conditions.
2. Some realistic equations for cracking pressures of concrete cover due to steel corrosion were derived in terms of α value (the degree of non-uniform corrosion) for various cover-to-bar diameter (c/d) ratios.
3. The present study indicates that the pressure to cause cracking of concrete cover due to corrosion expansion increases with an increase of cover depth and is almost linearly proportional to the cover-to-rebar diameter (c/d) ratio.
4. The cracking pressure of concrete cover decreases slightly as bar diameter increases. However, the effect of bar diameter on the cracking pressure due to steel corrosion is found to be rather small.
5. The cracking pressure of concrete cover increases as concrete strength increases. The regression equations were derived for the

cracking pressures as a function of compressive strength for various α values (non-uniform corrosion). It is noted that there exists fairly good correlation between cracking pressure and compressive strength.

6. The results of present analysis were compared with test data on the cracking pressure of concrete cover. It is confirmed that the results of present analysis agree very well with the test data.
7. Finally, the effect of non-uniform corrosion on the service life of concrete structures was discussed. It is noted that simple assumption of uniform corrosion may lead to unconservative estimation for service life.

References

[1] A. Costa, J. Appeleton, Chloride penetration into concrete in marine environment—Part I: main parameters affecting chloride penetration, Materials and Structures 32 (1999) 252–259.

[2] A. Costa, J. Appeleton, Chloride penetration into concrete in marine environment—Part II: penetration of long term chloride penetration, Materials and Structures 32 (1999) 252–259.

[3] B.H. Oh, S.Y. Jang, Prediction of diffusivity of concrete based on simple analytic equations, Cement and Concrete Research 34 (3) (2004) 463–480.

[4] B.H. Oh, S.Y. Jang, Effects of material and environmental parameters on chloride penetration profiles in concrete structures, Cement and Concrete Research 37 (1) (2007) 47–53.

[5] B.H. Oh, B.S. Jang, Chloride diffusion analysis of concrete structures considering the effects of reinforcements, ACI Material Journal 100 (2) (2003) 143–149.

[6] B.H. Oh, S.Y. Jang, Experimental investigation of the threshold chloride concentration for corrosion initiation in reinforced concrete structures, Magazine of Concrete Research 55 (2) (2003) 117–124.

[7] O.E. Gjoerv, Ø. Vennesland, Diffusion of chloride from seawater into concrete, Cement and Concrete Research 9 (2) (1979) 229–238.

[8] B.B. Hope, A.K.C. Ip, Chloride corrosion threshold in concrete, ACI Materials Journal 84 (4) (1987) 306–314.

[9] S.E. Hussain, A.S. Al-Gahtani, S. Rasheeduzzafar, Chloride threshold for corrosion of reinforcement in concrete, ACI Materials Journal 93 (1996) 534–538.

[10] M. Thomas, Chloride thresholds in marine concrete, Cement and Concrete Research 26 (4) (1996) 513–519.

[11] C. Andrade, C. Alonso, Corrosion rate monitoring in the laboratory and on-site, Construction and Building Materials 10 (5) (1996) 315–328.

[12] C. Andrade, C. Alonso, On-site measurements of corrosion rate of concretes, Construction and Building Materials 15 (2001) 141–145.

[13] J. Abdul-Hamid, J. Al-Tayyib, M.S. Khan, Corrosion rate measurements of reinforcing steel in concrete by electrochemical techniques, ACI Materials Journal 85 (2) (1988) 172–177.

[14] C. Arya, N.R. Buenfeld, J.B. Newmann, Assessment of simple methods of determining the free chloride content of cement pastes, Cement and Concrete Research 17 (6) (1987) 907–918.

[15] A. Castel, R. Francois, G. Arliguie, Factors other than chloride level influencing corrosion rate of reinforcement, in: V.M. Malhotra (Ed.), Proc. of CANMET/ACI Durability of Concrete, American Concrete Institute, Detroit, 2000, pp. 629–644.

[16] Q. T. Nguyen, S. Care, Y. Berthaud, A. Millard, F. Ragueneau, in press. Experimental and numerical behavior of reinforced mortar plates subjected to accelerated corrosion, *Int. J. Numer. Anal. Meth. Geomech*.

[17] O. Poupard, V. L'hostis, S. Catinaud, I. Petre-Lazar, Corrosion damage diagnosis of a reinforced concrete beam after 40 years natural exposure in marine environment, Cement and Concrete Research 36 (2006) 504–520.

[18] Y. Liu, Y., R. E. Weyer, Modeling of time-to-corrosion cracking in chloride contaminated reinforced concrete structures, ACI Materials Journal 95 (6) (1998) 675–681.

[19] B.H. Oh, K.H. Kim, B.S. Jang, Critical corrosion amounts to cause cracking of reinforced concrete structures, ACI Materials Journal 106 (4) (2009) 333–339.

[20] K.H. Kim, S.Y. Jang, B.H. Oh, Modeling mechanical behavior of reinforced concrete due to corrosion of steel bar, ACI Materials Journal 107 (2) (2010) 106–113.

[21] S.J. Williamson, L.A. Clark, Pressure required to cause cover cracking of concrete due to reinforcement corrosion, Magazine of Concrete research 52 (6) (2000) 455–467.

[22] M. Maage, S. Helland, E. Poulsen, O. Vennesland, J.E. Carlsen, Service life prediction of existing concrete structures exposed to marine environment, ACI Material Journal 93 (6) (1996) 602–608.

[23] K. Tuutti, Service life of structures with regard to corrosion of embedded steel, performance of concrete in marine environment, SP-65, American Concrete Institute (1980) 223–236.

[24] J.R. Clifton, L.I. Knab, Service life of concrete, Report No. NISTIR 89-4086, National Bureau of Standards, 1989.

[25] J.A. González, C. Andrade, C. Alonso, S. Feliu, Comparison of rates of general corrosion and maximum pitting penetration on concrete embedded steel reinforcement, Cement and Concrete Research 25 (2) (1995) 257–264.

[26] F.A. Oluokun, Prediction of concrete tensile strength from its compressive strength evaluation relations for normal weight concrete, ACI Materials Journal 88 (3) (1991) 302–309.

[27] A. Hillerborg, M. Modeer, P.E. Petersson, Analysis of crack formation and crack growth in concrete by means of fracture mechanics and finite elements, Cement and Concrete Research 6 (1976) 773–782.